AIAA JOURNAL
Vol. 35, No. 3, March 1997

Response of a Two-Dimensional Cascade to an Upstream Disturbance

Gerald C. Paynter*
The Boeing Company, Seattle, Washington 98124-2207

Time-accurate Euler simulations of the flow through two-dimensional cascades were used to provide data on the response of the flow entering a compressor to an upstream disturbance. These data were then used to evaluate several compressor face boundary condition hypotheses intended for supersonic inlet stability simulations. An accurate outflow boundary condition for time-accurate Euler/Navier–Stokes simulations of inlet flows is needed to determine the stability margin of an inlet that encounters an atmospheric disturbance. The boundary condition must provide an approximation of the response from the compressor when a disturbance from upstream passes through the inlet and into the compressor face. In the cascade analysis, the blade stagger angle, solidity, shape, and loading; axial Mach number; and disturbance strength were each varied through a representative range. It was found that the response of a cascade to an acoustic disturbance is almost nonreflective for blade geometry parameters characteristic of the compressor hub region and almost at a constant velocity condition for blade geometry parameters characteristic of the blade tip region. A convective (temperature) disturbance was also examined and was found to pass through a cascade without generating an upstream disturbance. Screen, constant Mach number, and constant velocity outflow boundary conditions were evaluated as possible compressor face boundary conditions. It is concluded that the constant velocity boundary condition is preferable to either the screen or the constant Mach number boundary conditions for inlet stability simulations.

Nomenclature

C	= blade chord length
M_{axial}	= axial Mach number before disturbance at inflow
P_t	= local total pressure
p	= local static pressure
S	= blade spacing
T_t	= local total temperature
u	= axial velocity
γ	= stagger angle, deg
σ	= solidity, C/S

Introduction

SUPERSONIC aircraft encounter atmospheric disturbances while in flight. If the propulsion system uses a mixed compression inlet to decelerate and compress the captured airflow for the engine, these disturbances can cause the shock system to be expelled from the inlet. This event is known as an inlet unstart. An unstart results in a serious loss of propulsive efficiency and can cause an asymmetric loading of the wing that could require large control surface forces to maintain aircraft control.

An atmospheric disturbance encounter is thought to result in (at least) acoustic and convective disturbances to the inlet flow. Acoustic disturbances are pressure disturbances that propagate downstream through the inlet at the local velocity plus the local speed of sound. Convective disturbances are temperature and density changes without an associated pressure change or velocity changes without an associated pressure change (a vorticity disturbance) that propagate downstream through the inlet at the local stream velocity. Both acoustic and convective disturbances eventually pass through the inlet and interact with the compressor.

Mixed compression supersonic inlets are designed to avoid inlet unstart (expulsion of the shock system) due to atmospheric and engine generated disturbances. The throat boundary-layer bleed system, throat slots and flow bypass systems, the inlet control system, the design value of the throat Mach number, and the position of the normal shock relative to the inlet throat are all used to achieve a sufficient stability margin to prevent unstart. Inlet stability measures, however, increase the inlet performance penalty, weight, complexity, and cost.

Time-accurate Euler/Navier–Stokes (ENS) simulations of the inlet flow subjected to disturbances are now being used to support the design of mixed compression inlets.[1,2] One goal of this analysis is to support the design of an inlet with a desired stability margin (unstart tolerance) while minimizing the performance penalty. Time-accurate ENS simulations of inlet flows are used to explore parametric variation of design parameters that affect inlet stability. The accuracy and, therefore, the usefulness of the ENS simulations depend on the accuracy of the boundary conditions used in the simulation. At the compressor face, the flow is subsonic and is about to enter the compressor. When acoustic and convective disturbances interact with the first stage of the compressor, reflected and transmitted disturbances result from this interaction. The reflected disturbance propagates back toward the inlet throat and can cause the inlet to unstart. The transmitted disturbances travel downstream through the blade passages, interact with the next compressor stage, and generate reflected disturbances throughout the later stages of the compressor.

The speed and memory available with current computers are insufficient to support the ENS simulation of the inlet/engine combination (at least in the context of a design study). Thus, the effect of the engine on the inlet flow is simulated through the selection of a boundary condition (the compressor face boundary condition) for unsteady time-accurate inlet flow analyses to investigate inlet stability issues. A number of compressor face boundary condition hypotheses have been put forward by various investigators.[3–7] Although at least one physical experiment[8] has been proposed for evaluation of the various compressor face boundary condition hypotheses, this or a similar experiment has not been performed as yet, and uncertainty exists about the accuracy of this boundary condition.

In lieu of a physical experiment such as that proposed by Sajben and Freund,[8] a time-accurate numerical study was performed with the NPARC[9] computer code, to investigate the interaction of acoustic and convective (temperature) disturbances with an unstalled cascade (a convective vorticity disturbance was not considered). The purpose of this study was to provide data for evaluation of the various compressor face boundary condition hypotheses over the range of axial Mach number, blade solidity, stagger angle, etc., of interest

Received June 11, 1996; revision received Nov. 23, 1996; accepted for publication Dec. 2, 1996; also published in *AIAA Journal on Disc*, Volume 2, Number 2.

*Associate Technical Fellow, Propulsion Research Unit, Commercial Airplane Group, Mail Stop 49-53, P.O. Box 3707. Associate Fellow AIAA.

at the compressor face and to use the data to evaluate several of the various outflow boundary condition hypotheses. Prior work on the interaction between an upstream disturbance and a cascade includes actuator disk and potential flow analyses by Kaji and Okazaki[10, 11] and an ENS simulation by Dorney.[12] Whereas Kaji and Okazaki considered a parametric variation of the geometric and flow parameters, the accuracy of their studies was unknown because of the assumptions used in their analyses. Dorney, on the other hand, considered just a single blade geometry in an ENS simulation.

Overall Approach

The goal of the current study was to guide selection of an appropriate outflow boundary condition for unsteady time-accurate ENS simulations of supersonic inlet flows where the effect of an upstream disturbance is considered. This goal was achieved in two phases. In the first phase, the flow through the compressor was approximated as the flow though a two-dimensional cascade. In the frame of reference of the moving blade, Euler simulations of axial acoustic and convective (temperature) disturbances were completed to obtain data on the response of the flow in the region upstream of the cascade to the passage of the disturbance through the cascade. In the second phase, screen, constant Mach number, and constant velocity outflow boundary condition hypotheses were evaluated through comparing the results of Euler analyses in a stationary frame of reference for a cylindrical duct subjected to acoustic and convective upstream disturbances, with the results from the cascade analysis.

Phase I Cascade Analysis Approach

The interactions of upstream acoustic and convective disturbances with a cascade were investigated by using unsteady and time-accurate two-dimensional Euler simulations of the flow through a cascade in the frame of reference of the moving blade. The radial velocity and radial gradients in flow properties were assumed to be negligible. With these assumptions, a stream surface through a compressor stage is cylindrical. If a stream surface is assumed to be unwrapped at a given radius, the result is a rectilinear cascade with an infinite number of blades.

In the first stage of a typical axial compressor, the stagger angle of the blade increases as a function of radius from about 20 deg at the hub to about 70 deg at the blade tip. The solidity also varies as a function of radius from about 3.0 at the hub to about 1.0 at the tip. Near the blade tip, the blade is almost flat (low camber) and has a low maximum thickness-to-chord ratio (at a given radius). Near the hub, the blade is highly cambered.

For acoustic disturbances, stagger angle, solidity, axial Mach number, blade loading, blade shape, and acoustic disturbance strength were varied over the range of interest or to explore the effect of a variation of a particular variable on the response of the flow upstream of the cascade to the passage of the disturbance through the cascade. A sketch of the interaction of an acoustic disturbance with a blade passage is shown in Fig. 1 just before a downstream traveling acoustic wave interacts with the blade passage. Just after the interaction between the disturbance and the blade passage, the flow is as sketched in Fig. 2. For convective disturbances, stagger angles of 20, 45, and 70 deg were considered for a single disturbance strength at a solidity of 1.0 and an axial Mach number of 0.5 for an unloaded blade.

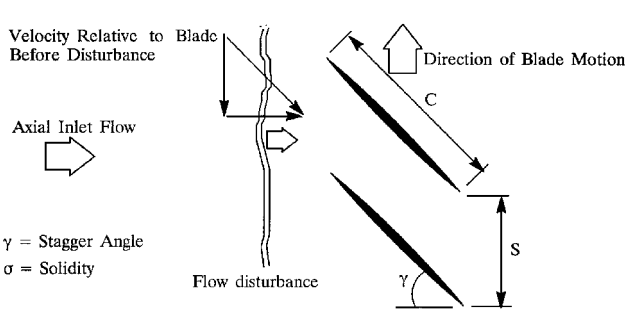

Fig. 1 Flow schematic prior to the disturbance/blade passage interaction: a disturbance approaches a blade pair from left.

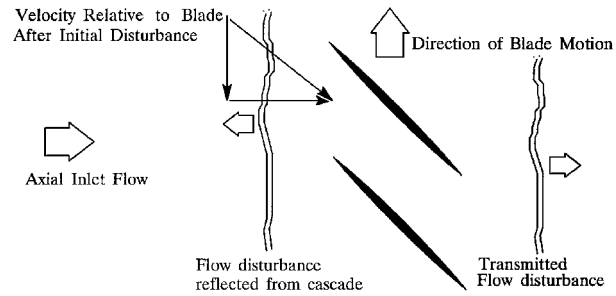

Fig. 2 Flow schematic after the disturbance/blade passage interaction: a reflected disturbance travels upstream to left.

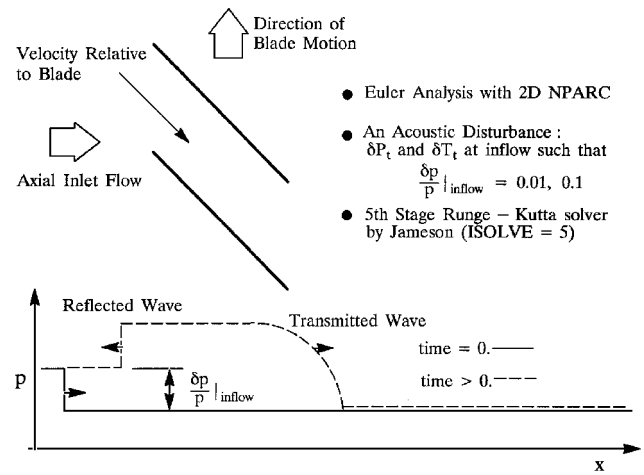

Fig. 3 Schematic of the cascade analysis with an acoustic disturbance.

After a steady-state flow had been achieved for a given cascade geometry, blade loading, and axial Mach number, an acoustic or convective disturbance was introduced at the inflow computational boundary as shown in Fig. 3 for an acoustic disturbance. In the time-accurate Euler simulations, the component of velocity in the direction of blade motion was assumed to be constant at the inflow boundary (equivalent to assuming the rotational speed of the blade is constant). The outflow boundary was placed far enough downstream that any disturbance from an interaction of the transmitted wave and the outflow boundary could not return and contaminate the solution just ahead of the blade passage. This is, in effect, an assumption that reflections from subsequent compressor or stator stages do not influence the flow ahead of the first compressor stage in the time scale of interest.

The assumptions implicit in the cascade analysis are summarized as follows. A time-accurate two-dimensional Euler analysis in the frame of reference of the cascade was used to predict how the flow just upstream of the cascade would change when a step disturbance was introduced at the inflow boundary in a plane parallel to the face of the cascade and allowed to propagate through the cascade. The flow through the cascade was assumed to be attached (unstalled) before and through the interaction with the disturbance. The tangential component of velocity at the inflow boundary was assumed to be constant (equivalent to an assumption that the rotational speed of the compressor is constant). For a flat blade of zero thickness, the effects of solidity, stagger angle, loading, axial Mach number, and disturbance strength were investigated parametrically (one circular arc blade geometry was also considered). The transmitted disturbance through the blade passage was assumed to have no influence on the flow ahead of the first cascade through propagation of reflections from the transmitted wave back through the blade passage. Acoustic and convective disturbances were considered. For the acoustic disturbance, changes in flow properties across the step disturbance were computed assuming that the change across the step is isentropic. The convective disturbance was assumed to be a change in static temperature without a change in static pressure. A convective vorticity disturbance was not considered.

Code Description

Two-dimensional time-accurate flow simulations were performed with the NPARC[9] ENS code, version 2.2 and the beta release of version 3.0. NPARC solves the Euler or Navier–Stokes equations in conservation law form on a multiblock body fitted grid system. An ideal gas, a Newtonian fluid, and the Fourier heat conduction law are assumed. The flow can be assumed to be laminar, turbulent, or inviscid; for a turbulent flow, a variety of turbulence models can be selected. A wide variety of boundary conditions are available and can be specified on any grid surface without restriction. A number of algorithms are available, and the user can select the one most appropriate for a particular application.

Flow simulations were performed in two steps. In the first step, a converged steady-state flow solution was achieved. In the second step, an acoustic or convective perturbation of known strength was introduced at the upstream boundary and allowed to propagate downstream and reflect from the cascade blade geometry.

The steady-state simulation to initialize the flowfield was done with the approximate factorization algorithm (ISOLVE = 1) using local time stepping (IVARDT = 2) with DTCAP = 1.0. Default values were used for the artificial dissipation coefficients: DIS2 = 0.25 and DIS4 = 0.64. Typically, about 2000 time steps were required to reduce the L_2 norm of the residual to about $(10)^{-7}$.

For the time-accurate calculations, a five step Jameson algorithm second-order accurate in time was selected (ISOLVE = 5). The time step throughout the grid block was set to a constant equal to the Courant–Friedrichs–Lewy (CFL) limit specified by DTCAP (IVARDT = 4 and DTCAP = 0.25) at the location of maximum change in the flow variables. This option is recommended in the user manual as providing the most rapid time-accurate simulation when tracking the physical time is not required. An evaluation of NPARC for time-accurate normal shock propagation simulations was reported by Paynter and Mayer.[13]

Grid and Geometry Description

The blade passage for the cascade parametric study was assumed to be 10 in. in length, and the computational domain extended 48 in. upstream and downstream of the blade passage in a single block grid, as shown in Fig. 4 (a stack of three grid blocks is shown). For most of the parametric study, the blades were assumed to be flat surfaces of zero thickness. A circular arc blade of zero thickness was also considered.

Computational grids were generated using the GRIDGEN2D[14] grid generation program. For both the cascade and screen studies, a uniform (unstretched) grid spacing was used in each coordinate direction. A grid refinement study was completed to ensure that the computed results for the strength of the reflected disturbance were independent of the grid density. Grids of 31×10, 64×10, 64×20, 64×15, and 130×30 were explored for use. A 64×20 grid was selected for use for most of the cascade simulations.

Boundary Conditions and Initial Conditions

A desired steady-state initial flow condition was established for each flow and geometry considered in the cascade study. The approximate factorization algorithm was used to establish the steady-state flow, as described in the Code Description section.

A freestream boundary condition (type 7) was used at the inflow plane, periodic boundary conditions (type 75) were used on the upper and lower surfaces of the computational domain ahead of and downstream of the blade passage, and a constant static pressure boundary condition (type 0) was used at the outflow boundary. Slip wall boundary conditions (type 50) were used on the walls of the blade passage. The outflow boundary was placed far enough downstream that the transmitted disturbance could not reflect from the outflow boundary and return to contaminate the solution in the region ahead of the blade passage where the strength of the reflected disturbance was determined.

The NPARC beta test release of version 3 recently became available. The type 75 periodic boundary condition in version 2.2 was replaced with a type 78 boundary condition in version 3.0. This boundary condition eliminates the need for a grid overlap on the periodic boundary and uses linear interpolation to determine property values on the boundary. Results for the strength of the reflected disturbance using this boundary condition were almost identical to those obtained with the type 75 boundary condition with NPARC version 2.2.

Disturbance Properties

Disturbances were always assumed to be a step change in flow conditions at the inflow boundary. The change in flow properties needed to introduce either an acoustic or a convective disturbance of desired strength was computed using a method described by Shapiro.[15] The acoustic disturbance was a step change in the properties across the disturbance computed assuming the changes in

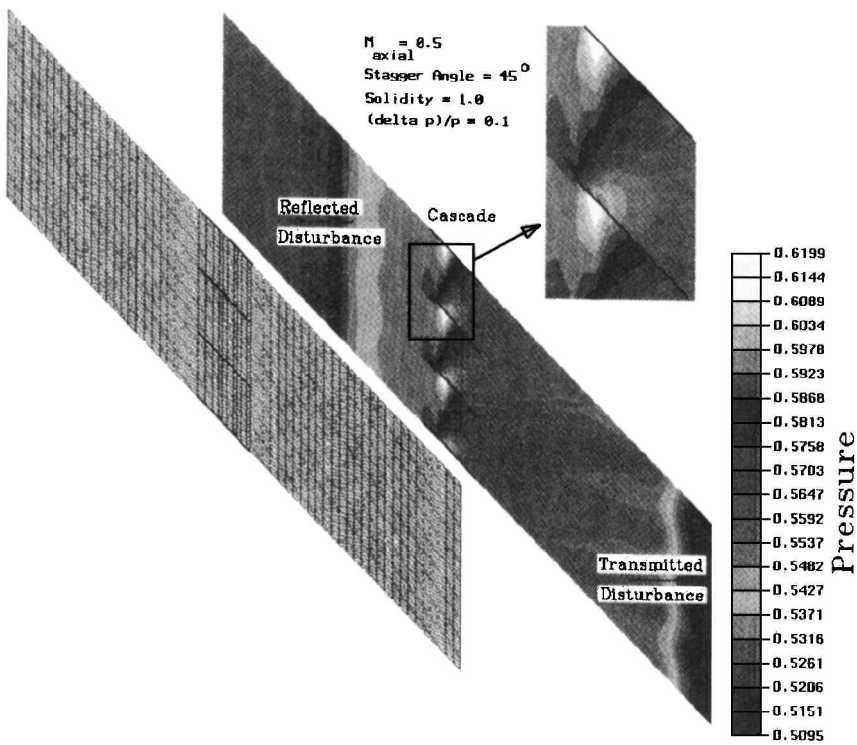

Fig. 4 Typical grid and pressure contour plot after reflection of an acoustic disturbance from the cascade.

properties across the disturbance were isentropic. The convective disturbance was a change in temperature without changes in pressure and velocity. In the text and figures that follow, changes to pressure or velocity for either the incident or the reflected disturbances are always normalized by the ambient pressure or velocity that existed before the incident disturbance.

Phase I Cascade Analysis Results

Acoustic Disturbances

A parametric numerical study was conducted to determine the strength of the reflected disturbance in the region upstream of the blade from the computed results as a function of blade solidity, stagger angle, axial Mach number, blade loading, camber, and acoustic disturbance strength. A contour plot of the predicted static pressure distribution through the computational domain after a $\delta p/p = 0.1$ static pressure disturbance has propagated through the region ahead of the blade passage, reflected and then propagated almost back to the inflow boundary, is shown in Fig. 4 for a stagger angle of 45 deg, a solidity of 1.0, and an axial Mach number of 0.5 for an unloaded blade (flow aligned with the blade passage). The flow pattern for a stack of three grid blocks is shown. Pressure and axial velocity color contour plots such as this were interrogated using a postprocessing code, GRIDVIEW, to determine properties behind the reflected disturbance in the region between the disturbance and the cascade leading edge. The flow properties in this region typically varied slightly, and this variation is reported in the discussion that follows.

The cascade parametric analysis results are plotted in Figs. 5–9. The variation in flow properties observed in the region upstream of the cascade and downstream of the disturbance at a given stagger angle is reported using symbols. Lines are linearly interpolated between stagger angles for a constant Mach number or solidity to show trends in the data.

The effect of stagger angle on the strength of the reflected disturbance for an unloaded blade (the flow is aligned with the blade passage prior to the disturbance) for a blade solidity of 1.0 and axial

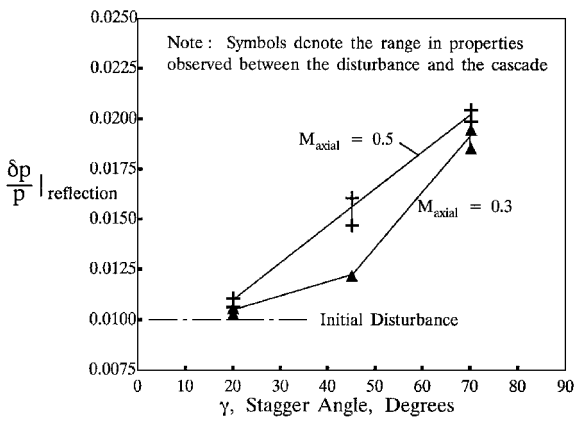

Fig. 5 Effect of M_{axial} on the reflected pressure; NPARC2D Euler simulation results solidity = 1.0.

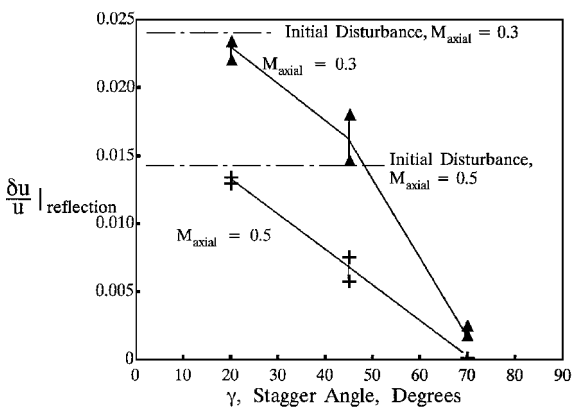

Fig. 6 Effect of M_{axial} on the reflected velocity; NPARC2D Euler simulation results solidity = 1.0.

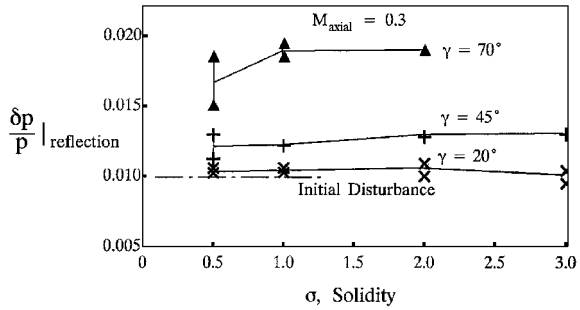

Fig. 7 NPARC2D Euler simulation results, effect of solidity.

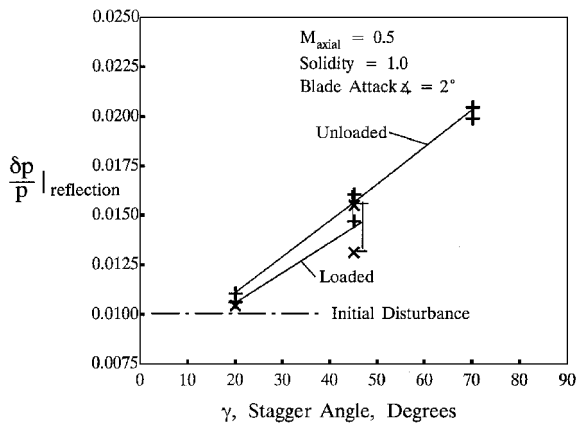

Fig. 8 NPARC2D Euler simulation results, effect of blade loading.

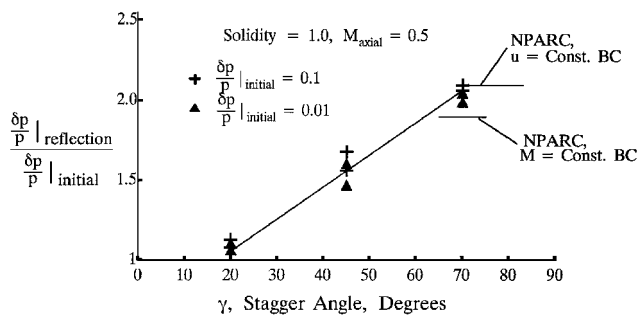

Fig. 9 NPARC2D Euler simulation results, effect of disturbance strength.

Mach numbers of 0.3 and 0.5 is shown for pressure and velocity in Figs. 5 and 6 ($\delta p/p = 0.01$). Whereas axial Mach number has some effect, stagger angle was found to have the greatest effect on the reflected disturbance strength. At a high stagger angle, the disturbance strength is consistent with that for a reflection of the disturbance from a solid wall moving with the stream velocity in the downstream direction. At low stagger angle, the reflected disturbance is weak and consistent with nonreflective interaction with the blade passage.

The effect of solidity on the reflected disturbance strength is illustrated for pressure in Fig. 7 for an unloaded compressor blade passage ($\delta p/p = 0.01$). In an actual compressor stage, the solidity would vary between 1 and 3. There was almost no variation in the strength of the reflected disturbance for solidities above 1. The strength of the velocity disturbance is not shown since it was found that the analysis of Shapiro[15] could be used to relate the strengths of the velocity and pressure disturbances.

The effect of blade loading on the strength of the reflected disturbance is illustrated in Fig. 8 for pressure for an axial Mach number of 0.5 and a 2-deg initial angle of attack on the blades ($\delta p/p = 0.01$). Blade loading was found to have only a weak influence on the strength of the reflected disturbance.

To explore the effect of camber, a circular arc blade shape was considered with a radius of curvature 1.3 times the chord length. For an axial Mach number of 0.5, a solidity of 1.0, $\delta p/p = 0.1$, 45-deg leading-edge angle, 0-deg trailing-edge angle, and with the

undisturbed flow aligned with the blade leading edge, the reflected pressure disturbance was about that found with a flat blade shape with a stagger angle of 20 deg and with the flow aligned with the blade passage.

The effects of the initial disturbance strength were examined by increasing the disturbance strength by a factor of 10 ($\delta p/p = 0.1$) for an axial Mach number of 0.5, a solidity of 1.0, and stagger angles of 20, 45, and 70 deg. The results for the strength of the reflected pressure disturbance normalized by the strength of the initial disturbance are shown in Fig. 9. The normalized change in pressure was found to be independent of disturbance strength and to vary almost linearly with stagger angle between 20 and 70 deg. The strength of the reflected disturbance is a linear function of the strength of the incident disturbance for the range of disturbances considered. The change in velocity is not shown because pressure and velocity changes can be related through the analysis of Shapiro,[15] as noted earlier.

Convective Disturbances

Convective disturbances were also examined for blade passages with stagger angles of 20, 45, and 70 deg, an axial Mach number of 0.5, and a solidity of 1.0 (unloaded blade). The convective disturbance was an increase in the local static temperature at the inflow plane of 2.9% (the same increase in static temperature as would be caused by an acoustic disturbance with a $\delta p/p = 0.1$ increase in static pressure). As expected, the convective disturbance caused no reflected wave as it passed through the blade passage at the three stagger angles examined.

Discussion

The assumption in the current study that the wave transmitted through the blade passage does not interact with subsequent compressor and/or stator stages and cause a delayed response of the inlet flow at the compressor face was also examined for several cascade geometries at an axial Mach number of 0.5. An acoustic disturbance was introduced at the outflow boundary of the cascade analysis domain and allowed to propagate upstream and reflect from the downstream face of the cascade. For both $\delta p/p = 0.01$ and 0.1 pressure disturbances, there was no wave transmitted from downstream of the cascade through the blade passage to the inlet flow in the time it took the disturbance reflected from the downstream blade surface to propagate back to the outflow boundary. This effect was also observed in an ENS simulation of the flow through a blade passage by Dorney.[12] Dorney attributed this phenomenon to acoustic blockage, inhibition of the upstream propagation of acoustic disturbances in a transonic flow. For an axial Mach number and a blade geometry that would result in a transonic flow in the blade passage, this effect could isolate the inlet from disturbances propagating upstream through the blade passages of the first stage. Because understanding acoustic blockage was not the objective of the current work, the current results on this are interesting but incomplete. Acoustic blockage and the influence of the blade geometry and flow properties on it should be investigated further in a systematic study.

Phase II Boundary Condition Evaluation Approach

Once the data from the cascade analysis study were available, they were used to evaluate several of the proposed compressor face boundary condition hypotheses. NPARC was again used to generate data for boundary condition evaluation by considering the flow through a cylindrical duct (now in a stationary frame of reference). Using an Euler analysis, a steady uniform axial flow was established in the cylindrical duct at a desired axial Mach number. The boundary condition to be evaluated as a possible compressor face boundary condition was then imposed at the outflow boundary, and either a convective or an acoustic disturbance of known strength was introduced at the inflow boundary. In a time-accurate, unsteady Euler simulation of the duct flow, sufficient time steps were taken to allow the disturbance to propagate across the domain, through the outflow boundary, and generate a reflected disturbance that propagated far enough upstream that the strength and properties of this wave could be determined. These simulation results for the properties between the outflow boundary and the reflected wave were then compared with the results from the cascade analysis. Conclusions could then be made about the ability of a given boundary condition to simulate the effect of the compressor on the inlet flow.

The NPARC screen, constant Mach number, and constant velocity boundary conditions were considered as possible compressor face boundary conditions. Screens have been used at the inlet outflow boundary in steady-state subsonic inlet experiments[16] to simulate the effect of the compressor on the inlet flow. Constant Mach number[4] and constant velocity[3] outflow boundary conditions have also been proposed as compressor face boundary condition hypotheses. These were examined by comparing results from time-accurate ENS simulations of a cylindrical duct at an initial axial Mach number of 0.5 subjected to acoustic and convective disturbances with results from the cascade parametric study.

Code Description

Two-dimensional time-accurate flow simulations were performed with the NPARC[9] ENS code, version 2.2 and the beta release of version 3.0, as described in the Phase I Cascade Analysis Approach.

Flow simulations were performed in two steps. In the first step, a converged steady-state flow solution was achieved. In the second step, an acoustic or convective perturbation of known strength was introduced at the upstream boundary and allowed to propagate down a cylindrical duct and interact with the outflow boundary.

The steady-state simulation to initialize the flowfield was done with the approximate factorization algorithm (ISOLVE = 1) using local time stepping (IVARDT = 2) with DTCAP = 1.0. Default values were used for the artificial dissipation coefficients. Typically, about 2000 time steps were required to reduce the L_2 norm of the residual to about $(10)^{-7}$.

For the time-accurate calculations, a five step Jameson algorithm second-order accurate in time was selected (ISOLVE = 5). The time step throughout the grid block was set to a constant equal to the CFL limit specified by DTCAP (IVARDT = 4 and DTCAP = 0.25) at the location of maximum change in the flow variables.

Grid and Geometry Description

The cylindrical duct for the boundary condition evaluation had a radius of 19 in. and a length of 94 in. A 95 $\times$ 20 grid was used for the boundary condition evaluation studies (not shown).

Boundary Conditions and Initial Conditions

For the cylindrical duct used for the boundary condition evaluation studies, the total pressure and temperature at the inflow boundary were specified (type 0), the upper wall was taken as a slip surface (type 50), and the lower wall was assumed to be an axis of symmetry (type 51).

For the screen boundary condition, the screen was placed at about half of the axial length of the cylindrical computational domain using the NPARC screen boundary condition option, type 58. The static pressure was specified at the outflow boundary (type 0), and this pressure was iterated until the desired Mach number in the duct was achieved (or the screen choked).

For the constant Mach number and constant velocity outflow boundary conditions, the total pressure and temperature at the inflow boundary were specified (type 0), the upper wall was taken as a slip surface (type 50), and the lower wall was assumed to be an axis of symmetry (type 51). The outflow boundary was assumed to be either a constant Mach number or constant velocity boundary condition (both type 97).

Disturbance Properties

Disturbances were always assumed to be a step change in flow conditions at the inflow boundary and were computed using a method described by Shapiro.[15]

Phase II Boundary Condition Evaluation Results

NPARC screen (type 58), constant Mach number (type 97), and constant velocity (type 97) outflow boundary conditions were evaluated for possible use as the compressor face boundary condition for inlet unsteady flow simulations. A cylindrical flow domain was established with a uniform axial flow at a desired Mach number.

The boundary condition to be evaluated was imposed at the outflow boundary of this domain, and either a convective (temperature) or acoustic disturbance of known strength was introduced at the inflow boundary. The disturbance was allowed to propagate across the domain, through the outflow boundary, and generate a reflected disturbance that propagated far enough upstream that the strength and properties of this wave could be determined. The cylindrical duct simulation results for the properties between the outflow boundary and the reflected wave were then compared with the results from the cascade analysis.

Screen Boundary Condition

The NPARC screen boundary condition was found to be inadequate for representing the wave reflection response to an acoustic disturbance for the midspan to tip region of a compressor blade because a strong response characteristic of the blade geometry in the midspan to tip region of a compressor requires a low screen porosity. The screen outflow boundary chokes at a flow rate through the boundary that is a function of the porosity. It was impossible to match the strength of the reflected disturbance (as obtained from the cascade analysis described) and get desired axial Mach numbers (on the order of 0.5) for higher stagger angles with the NPARC screen boundary condition. The strength of the wave reflection as a function of screen porosity at an axial Mach number of 0.3 is shown in Fig. 10. It appears that a screen could be used to represent a cascade with a low stagger angle. This suggests that an actuator disk model, which is similar to a screen model but with an increase rather than a decrease in total pressure across the disk surface, may be useful as a way to represent the compressor outflow boundary condition.

Constant Mach Number Boundary Condition

For the NPARC constant Mach number outflow boundary condition, the acoustic disturbance test case had an initial axial Mach number of 0.5 and a $\delta p/p = 0.1$ static pressure disturbance. The NPARC constant Mach number boundary condition held the Mach number at the outflow plane to within 0.005% of the value specified once the disturbance front had propagated away from the outflow plane a few grid points. The predicted change in pressure downstream of the wave reflection from the boundary normalized by initial pressure disturbance was equal to 1.88. A comparison of the cascade results with the NPARC constant Mach number boundary condition results for the strength of the reflected pressure disturbance (as shown in Fig. 11) suggests a constant Mach number outflow boundary condition would represent the interaction of an acoustic wave with a cascade at a stagger angle of about 60 deg.

For the convective disturbance test case, the initial axial Mach number was again 0.5. The freestream static temperature was increased by an amount equal to that which would occur with a $\delta p/p = 0.1$ static pressure disturbance, about 3%. The cascade analysis results indicated that a convective disturbance should pass through the outflow boundary without generating an acoustic disturbance that is propagated upstream. The NPARC constant Mach number boundary condition did, however, generate a 1% decrease in static pressure disturbance that propagated upstream from the boundary as a result of the convective disturbance passing out through the boundary.

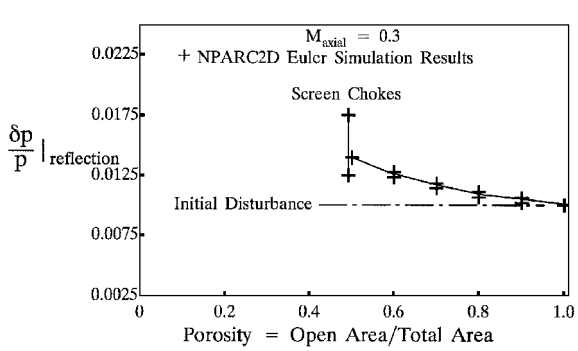

Fig. 10 Results from the NPARC screen boundary condition.

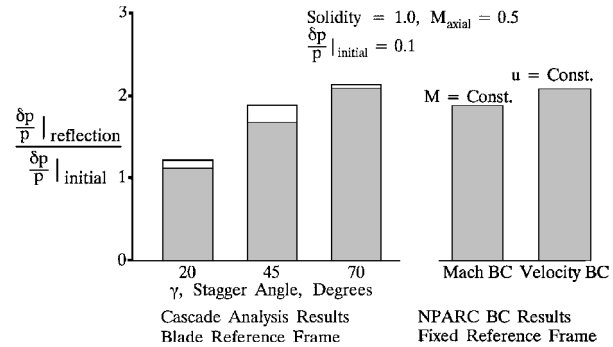

Fig. 11 Comparison of cascade analysis results and NPARC constant Mach number and constant velocity boundary condition results for an acoustic disturbance.

Thus, although the NPARC constant Mach number boundary condition is definitely within the correct range for acoustic disturbances from comparison with the cascade analysis results, its use results in a pressure disturbance at the boundary inconsistent with the cascade results when a convective disturbance passes through the boundary.

Constant Velocity Boundary Condition

For the NPARC constant velocity outflow boundary condition, the test cases for evaluating the interaction of acoustic and convective disturbances were the same as for the constant Mach number boundary condition already discussed. For a $\delta p/p = 0.1$ static pressure acoustic disturbance, the NPARC constant velocity boundary condition held the velocity to within 0.05% of the desired value. The predicted change in pressure downstream of the wave reflection from the boundary normalized by initial pressure disturbance was equal to 2.086. A comparison of the cascade results with the NPARC constant velocity boundary condition results for the strength of the reflected pressure disturbance (as shown in Fig. 11) suggests a constant velocity outflow boundary condition would represent the interaction of an acoustic wave with a cascade at a stagger angle of about 70 deg.

For the convective disturbance test case, the cascade analysis results indicated that a convective disturbance should pass through the outflow boundary without generating an acoustic disturbance that is propagated upstream. The NPARC constant velocity boundary condition did not generate an acoustic disturbance that propagated upstream from the boundary as a result of the convective disturbance passing out through the boundary.

The NPARC constant velocity boundary condition is definitely within the correct range in the strength of the reflected disturbance for acoustic disturbances in comparison with the cascade analysis results. No pressure disturbance is generated at the boundary when a convective disturbance passes through the boundary, which is consistent with the cascade results. For this reason, the NPARC constant velocity boundary condition should be more accurate than the NPARC constant Mach number boundary condition for inlet stability simulations where both convective and acoustic disturbances are present.

Conclusions

Time-accurate Euler simulations with the NPARC code were used to provide data on the interaction of acoustic and convective (temperature) disturbances with a compressor cascade. It was found that the strength of the reflected wave from an acoustic disturbance is a strong function of axial Mach number and stagger angle and a weak function of blade loading, camber, and solidity for solidities of one and above. The strength of the wave reflection varies from almost nonreflective for a stagger angle consistent with the hub (20 deg) to almost constant velocity for a stagger angle consistent with the blade tip (70 deg). Convective disturbances were found to pass through the outflow boundary without generating an upstream disturbance from the boundary.

The screen boundary condition option within NPARC was found to be inadequate for representing the response of the flow upstream of a cascade to an acoustic disturbance because a strong response consistent with a high stagger angle requires a low screen porosity. The NPARC screen model chokes for duct flow rates of interest when the porosity is low, however, so that it is impossible to specify the low porosity needed to represent higher stagger angles and get axial Mach numbers of interest.

The NPARC constant Mach number outflow boundary condition was found to be approximately correct in the strength of the pressure disturbance from the boundary that results from an acoustic disturbance passing through the outflow boundary. A convective (temperature) disturbance passing through the outflow boundary with this boundary condition, however, generated a pressure disturbance from the boundary inconsistent with the cascade results. This could be misleading in the use of unsteady ENS analysis to evaluate inlet stability margin.

The NPARC constant velocity outflow boundary condition was also found to be approximately correct in the strength of the pressure disturbance from the boundary that results from an acoustic disturbance passing out through the boundary. A convective (temperature) disturbance passing through the outflow boundary with this boundary condition did not generate a pressure disturbance from the boundary. For inlet stability simulations, the NPARC constant velocity outflow boundary condition should be selected in preference to the constant Mach number boundary or screen boundary conditions.

The cascade analysis showed that the compressor stage or fan stage response to an upstream disturbance is a function of the local blade properties (solidity and stagger angle) and the axial Mach number. Of the simple compressor face boundary conditions evaluated, the constant velocity boundary condition is preferred. A compressor face boundary condition in which the response to a disturbance is a function of the local blade properties and upstream flow has yet to be developed but is needed to improve the accuracy of supersonic inlet unstart simulations.

Acknowledgments

The author would like to thank S. F. Birch, R. Decher, R. M. Hearsy, J. S. Lee, L. T. Clark, D. W. Mayer, T. A. Reyhner, and M. Sajben for their comments on the work; G. D. Power for his help with NPARC; and J. P. Lewis for his help with display of the computed results.

References

[1]Hedges, L., Lewis, J., Carlin, C., and Beck, C., "Supersonic Inlet Simulation with Closed Loop Control and Moving Control Surfaces," AIAA Paper 96-0493, Jan. 1996.

[2]Cole, G. L., Melcher, K. J., Chicatelli, A. K., Hartley, T. T., and Chung, J. K., "Computational Methods for HSCT-Inlet Controls/CFD Interdisciplinary Research," AIAA Paper 94-3209, June 1994.

[3]Mayer, D. W., and Paynter, G. C., "Prediction of Supersonic Inlet Unstart Caused by Freestream Disturbances," *AIAA Journal*, Vol. 33, No. 2, 1995, pp. 256–275.

[4]Chung, J., and Cole, G. L., "Comparison of Compressor Face Boundary Conditions for Unsteady CFD Simulations of Supersonic Inlets," AIAA Paper 95-2627, July 1995.

[5]Clark, L. T., "Dynamic Response Characteristics of a Mixed Compression Supersonic Inlet as Part of a Larger System," AIAA Paper 95-0036, Jan. 1995.

[6]Chung, J. K., "Numerical Simulation of a Mixed Compression Supersonic Inlet Flow," AIAA Paper 94-0583, Jan. 1994.

[7]Decher, R., Mayer, D. W., and Paynter, G. C., "On Supersonic Inlet-Engine Stability," AIAA Paper 94-3371, June 1994.

[8]Sajben, M., and Freund, D. D., "Experimental Exploration of Compressor-Face Boundary Conditions for Unsteady Inlet Flow Computations," AIAA Paper 95-2886, July 1995.

[9]Cooper, G. K., and Sirbaugh, J. R., "The PARC Code: Theory and Usage," Arnold Engineering Development Center, AEDC-TR-89-15, Arnold AFB, TN, Dec. 1989.

[10]Kaji, S., and Okazaki, T., "Propagation of Sound Waves Through a Blade Row: I. Analysis Based on the Semi-Actuator Disk Theory," *Journal of Sound and Vibration*, Vol. 11, No. 3, 1970, pp. 339–353.

[11]Kaji, S., and Okazaki, T., "Propagation of Sound Waves Through a Blade Row: II. Analysis Based on the Acceleration Potential Method," *Journal of Sound and Vibration*, Vol. 11, No. 3, 1970, pp. 355–375.

[12]Dorney, D., "Unsteady Acoustic Wave Propagation in a Transonic Compressor Cascade," AIAA Paper 96-0246, Jan. 1996.

[13]Paynter, G. C., and Mayer, D. W., "Evaluating the Temporal Accuracy of Inlet Normal Shock Propagation Simulations," *AIAA Journal*, Vol. 33, No. 8, 1995, pp. 1534–1536.

[14]Steinbrenner, J. P., Chawner, J. R., and Fouts, C. L., "The GRIDGEN 3D Multiple Block Grid Generation System," General Dynamics Corp., WRDC-TR-90-3022, Vols. 1 and 2, Fort Worth, TX, July 1990.

[15]Shapiro, A. H., *The Dynamics and Thermodynamics of Compressible Fluid Flow*, Vol. 2, Ronald, New York, 1954, Chap. 23.

[16]Boldman, D. R., Iek, C., Hwang, D. P., Larkin, M., and Schweiger, P., "Effect of a Rotating Propeller on the Separation Angle of Attack and Distortion in Ducted Propeller Inlets," AIAA Paper 93-0017, Jan. 1993.

S. Fleeter
Associate Editor